EJTAS
ISSN 2786-7447
EUROPEAN JOURNAL OF THEORETICAL AND APPLIED SCIENCES
OPEN ACCESS
PEER REVIEWED

Deep Learning Models for Classification of Lung Diseases

Mazhar Javid
Department of software Engineering Taiyuan University of Technology Taiyuan 030024, Shanxi, China
Hongwei Xie
Department of software Engineering Taiyuan University of Technology Taiyuan 030024, Shanxi, China

Suggested Citation
Javid, M., & Xie, H.(2024). Deep Learning Models for Classification of Lung Diseases. *European Journal of Theoretical and Applied Sciences, 2*(2), 858-868.
DOI: 10.59324/ejtas.2024.2(2).77

Abstract:

This thesis focuses on the importance of early detection in lung cancer through the use of medical imaging techniques and deep learning models. The current practice of examining nodules larger than 7 mm can delay detection and allow cancerous nodules to grow undetected. The project aims to detect nodules as small as 3 mm to improve the chances of early cancer identification. The use of constrained volume datasets and transfer learning techniques addresses the scarcity of medical data, and deep neural networks are employed for classification and segmentation tasks. Despite the limited dataset, the results demonstrate the effectiveness of the proposed models. Class activation maps and segmentation techniques enhance accuracy and provide insights into the most critical areas for diagnosis. This research contributes to the understanding of lung disease diagnosis and highlights the potential of deep learning in medical imaging.

Keywords: *Lung disease classification, Transfer learning, Deep learning, Image analysis, Diagnostic accuracy.*

Introduction

Lung cancer is an uncontrollable growth of anomalous cells in either the lungs or both. This prevents the heart from working correctly, and thereby prevents the liver from completely nourishing the body with oxygen (Warburg, & Nguyen, 2015). Those anomalous cells will continue to replicate until a tumor forms. Such tumors may be benign, staying in one location, or they can be malignant, spreading across the body through the bloodstream or other means (Nery, 2012). (What Is Lung Cancer? n.d.) Nodules in the lungs exist in a range of sizes, with focal sizes ranging from 3 mm to 30 mm (Pierce, & Damjanov, 1998). A nodule measuring less than 3 mm is referred to as a micro nodule, while anything larger than 30 mm is considered a mass (Faguet, 2016). CT imaging is now possible to visualize very small or low-contrast nodules that are challenging to identify on conventional radiograms (Raza, 2019). The popular method for identifying lung nodules is close examination of the CT images by a professional radiologist. Since 1980, numerous attempts have been made to create an automated system that can quickly and cheaply identify lung nodules (Dhama, Chauhan, & Singhal, 2005). While neither system is entirely successful in automatically locating lung nodules, other methods have significantly reduced the workload of radiologists (Del Piccolo, et al., 2021). These systems are frequently categorized as CAD (Computer-Assisted Diagnostic) systems. Since the focal point of this paper is on the classification of lung cancer or lung disease (pneumonia and tuberculosis), I'll start with a quick overview of certain screening methods. All ofthe procedures rely on radiography, a once-

outdated medical imaging technique. However, developments in digital technology of machine learning and have resurrected this procedure (Arbib, 2003) and its significance in the diagnosis of pulmonary illness (Suzuki, 2012). In particular, they enable the detection of various cardiothoracic lessons on x-ray imaging. A notable accomplishment is the increased acceptance of machine learning models in medical diagnosis, which is related to their accuracy and improves disorder detection.

Discussion on Deep Learning Lung Nodule Detection

$$Sensitivity = \frac{TP}{TP+FN} \quad (1)$$

There is a large amount of literature available for detecting and segmenting lung nodules from 2D and 3D CT images. Every paper follows specific steps in an algorithmic framework. Some of the steps, found in most articles, are popular. These specific steps include the acquisition of photos, preprocessing, segmentation of the lungs, nodule identification, and false positive reduction. Creating an image of the lung is the initial step in the procedure. There are several public repositories available for research, such as the Early Lung Cancer Action Program (ELCAP), the Reference Image Database to Evaluate Therapy Response (RIDER), the Lung Image Database Consortium (LIDC), and the Lung Image Database Consortium and Image Database Resource Initiative (LIDC-IDRI). Many researchers have also utilized numerous private databases accessible through partner hospitals. The second stage of lung segmentation is called preprocessing, which reduces noise and artifacts in CT images. Preprocessing procedures may also be necessary due to variations in image sizes and intensities produced by different CT scanners. These precautions are not necessary in all cases, and as a result, not all papers mention pre-processing. Lung segmentation is the third step, involving the division of the lung region into its muscle and fat tissue portions. The two main categories of lung segmentation techniques are threshold-based and shape- or edge-based techniques.

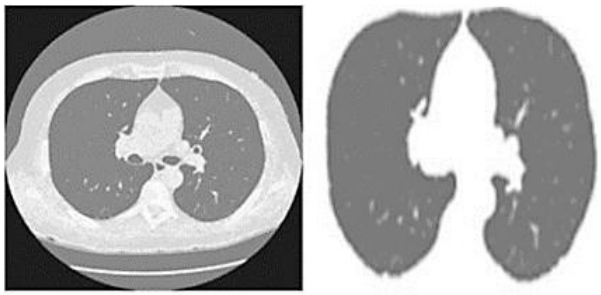

Figure 1. CT SCAN after Threshold Technique Applied

Pixel / Voxel-Based Machine Learning

Powerful computers capable of computation are becoming increasingly common, paving the way for new technologies in medical image analysis and processing, including pixel/voxel-based approaches. This approach directly utilizes voxel/pixel values in input images instead of generating features from segmented areas. Consequently, neither feature extraction nor segmentation is required. Due to its avoidance of errors caused by improper segmentation and feature extraction, PML's performance.

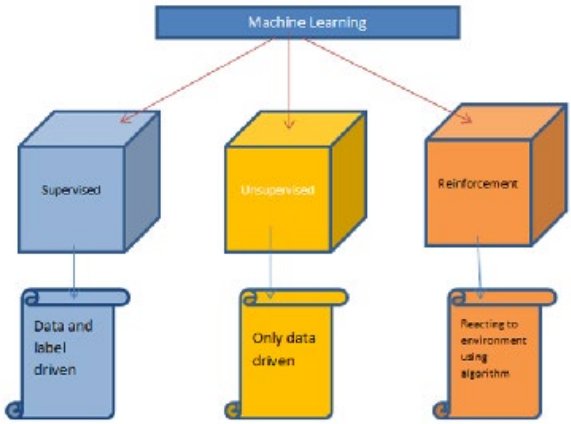

Figure 2. Machine Learning Method

MTANs are Used to Separate Bone from Soft Tissue in Chest Radiographs (CXRs)

When analyzing medical pictures for various lung disorders such as pneumonia or TB, a chest X-Ray is quite possibly the most usually used determination. In the United States, north of 1 million people require hospitalization because of pneumonia every year, with roughly 50,000 people dying as a result (Jaeger, et al., 2013). Lung nodule CSR screening has the potential to overlook illnesses like lung cancer. In retrospect, though, not all of them are obvious. According to studies, ribs or clavicles hid at least partially 83-94 percent of lung cancer patients. Insulae-energy imaging, a method for taking pictures of two tissues, was studied. You'll require a "soft-tissue" image and a "bone" image to solve this issue (Lo, et al., 1995b). There are many drawbacks to this therapy. Radiation exposure is, nonetheless, one of the most significant.

The MTANN models were developed to overcome this issue and to identify ribs from soft tissue. The goal of the training is to provide dual-energy radiography images of bone and soft tissue to those algorithms. As shown in Figure 2-1, CXRs and matching boneless photos were used to train the MTANN. The model's performance on the hidden image data is shown. Please refer to Figure 2-2. In the final image, the artifacts are considerably diminished, but soft tissue components like lung veins remain preserved.

The Spatial Interdependence Matrix is a visual pattern that may be used to evaluate damaged photographs. If the image is not destroyed, the weights are distributed toward the matrix's diagonal. Otherwise, depending on the structure's state, numerous patterns emerge. The fibrosis SIM pattern differs from one healthy lungs imaging to the next when it comes to lung disorders. Fibrosis formations can be observed all across the lungs, whereas healthy lungs contain a minimal number of structures.

A bunch of boundaries from the Spatial Interdependence Matrix is utilized to explore the primary characterization of lung images (correlation, chi-square, and inverse difference moment). Based on prior information that CT scans exhibit fuzzy forms, the authors of Lo, et al., (1995a) utilize a gaussian kernel to convolve the inputs. The Spatial Interdependence Matrix was created with a total of 64 grey levels.

CXR Screening System that Work Automatically

This procedure employs a multistage processing technique based on a theoretical framework in Nebauer, C. (1998) (see Figure 2-3), which initially segments images before attempting to forecast a disease shown on CXRs using a combination of texture and form data. The algorithm employs the same reasoning as radiologists when assessing the lungs, which involves comparing the functions of the right and left lung. The form features to focus on include important geometrical qualities, whereas the texture features describe the inner lungs region. The presented approach in Section 3 includes three stages: segmentation comes first, then feature extraction, and finally classification, in that order. The initial phase consists of three sections. The first is content-based picture retrieval, which employs a partial Radon transform and the Bhattacharyya shape similarity measure. Then, using SIFT-flow, a patient anatomical model of the lung shape is created by Loog, et al (2006). At the end, a graph cut optimization strategy is used to remove lung borders. Textural characteristics of the segmented lungs are retrieved using features such as the intensity histogram, gradient magnitude, a histogram of directed gradients, and other features. The last model used for classification is a Support Vector Machine (SVM) (Loog, et al., 2006).

Findings of the Research

Approaches to chest X-Rays Analysis Using Deep Learning

In latest Deep Neural Networks (Oda, et al., 2009; Ramalho, et al., 2014; Aherne, et al., 1998; Beylkin, 1987) applications have resulted in significant advancements in medical imaging. The effectiveness of dimensionality reduction procedures such as lung segmentation was proved in the Chest X-Ray image analysis (Liu, Yuen, & Torralba, 2010). On relatively limited data sets, we employed deep learning

segmentation and classification algorithms (Liu, Yuen, & Torralba, 2010) to enhance TB diagnosis. (103 photos per class). The purpose of the research is to further investigate these strategies. Findings and Results are shown which concentrate on various deep learning algorithms for lung disease classification.

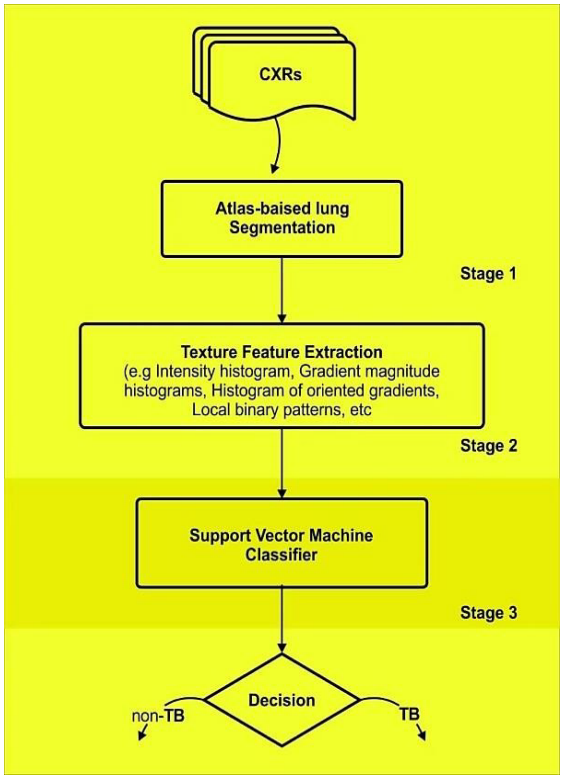

Figure 3. The TB Screening System that was Created is Described

Data Augmentation

Data augmentation is a method used to expand a training dataset by generating fictitious new samples from existing ones. The issue of restricted data availability, which can hinder the effectiveness of machine learning models, is frequently addressed in the field of medical imaging through data augmentation. Medical photos can be enhanced using techniques such as rotation, flipping, scaling, cropping, and noise addition to create new images that are similar to the originals but with slight differences. This approach reduces overfitting and helps the model learn to generalize to new data more effectively. Moreover, training a reliable machine learning model can be challenging due to varying orientations, resolutions, and levels of noise in medical images. By employing data augmentation approaches, we can simulate various imaging scenarios and ensure that the model is capable of consistently detecting and classifying features across different image formats. Overall, data augmentation can assist in enhancing the robustness and accuracy of machine learning models trained on medical images, thereby increasing their dependability for clinical applications.

Dataset

Pneumonia is a bacterial infection that affects the alveoli, or small air sacs in the lungs. Common symptoms include a dry cough, breathing difficulties, chest discomfort, with a fever. The collection, titled "Labeled Optical Tomography and Chest X-Ray Images for Classification", contains pictures of patients from the Guangzhou Medical Center (Kostopoulos, et al., 2018). It includes information that is separated into two categories: normal data and pneumonia-related data. The information is fully based on the patient's usual clinical treatment. For our study, I wanted to keep the dataset small and uniformly distributed., despite the fact that it comprises hundreds of confirmed OCT and X- Ray images., therefore only 153 images Ire picked at random from the resources designated as healthy and 306 images from the tuberculosis collection.

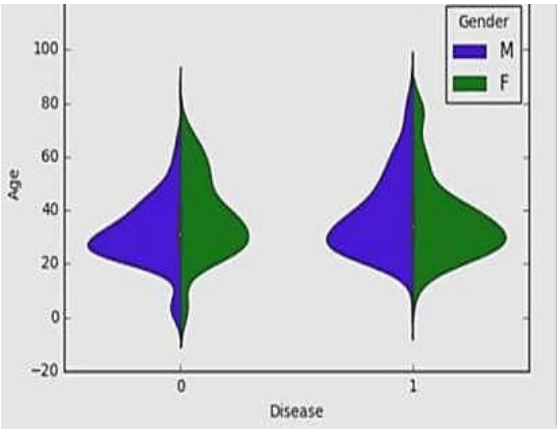

Figure 4. Combined Distribution of Genders and Ages among Images

To extract lungs information and eliminate exterior areas, I used the manually made masks that came with the SH dataset extension, especially the segmented SH dataset. Even though, when compared to the picture area distribution, it has a distribution that is quite close to the conventional one. The segmentation data reveals a significant amount of heterogeneity due to the lack of consistent boundaries and lung shapes as shown in Figures 2-5.

Evaluation

All projects require the assessment of a machine learning model. When it comes to the efficacy of classifiers, one measure may not be sufficient. Therefore, I will utilize the following measures in this thesis: exactness, F1-score, accuracy, responsiveness, explicitness, a graphical presentation - ROC (Receiver Operating Characteristic) curve, and AUC (Area under the Curve) (Area under the ROC curve). In this section, I define metrics for binary issues. To adapt it for a three-class case, I compute them per label using the "one versus the others" technique (Liu, et al. 2018). The total number of figures is divided by the quantity of successfully classified items, which gives the overall number of predictions.

Figure 5. A and B Example of an Original Scan in Dataset of SH Left and Segmented Output Right

Convolutional Neural Network

After the publication of AlexNet, as described by [25] in 2012, convolutional neural networks (CNN) rekindled interest in the scientific community. In computer vision tasks, CNNs, and later deep models like VGG (He, et al., 2016), have proven to be highly useful. According to published research, these models demonstrate significantly better capture of distinct aspects, such as changes in gradients, when compared to conventional algorithms that heavily rely on various feature engineering techniques. CNN is composed of several convolution layers followed by pooling operators in a traditional convolutional neural network architecture for classification. Kernels, which are small sensors that process input and output data, are used to construct the convolution layers. Upper layers (hidden) can detect more complex information such as rectangles or circles based on the received input, allowing them to better comprehend it. These operators can successfully capture an image's spatial and temporal dependencies, allowing them to learn various local features such as straight lines (horizontal or vertical) and curves. A network learns more "abstract" combinations as input is processed through higher layers.

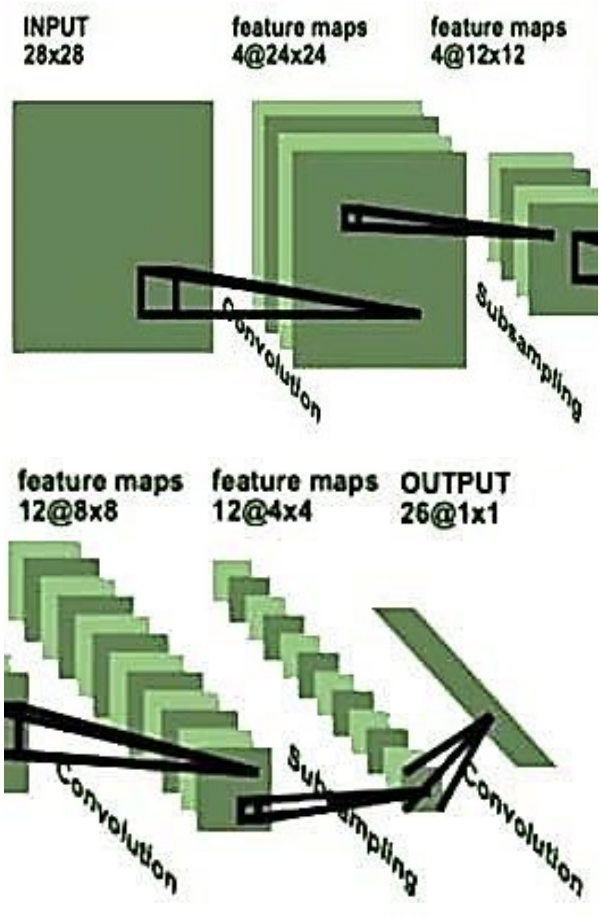

Figure 6. Image Processing with a Convolutional Neural Network

Transfer Learning in Lung Cancer Classification

Transfer Learning

It is possible to improve the training process by using tools that have already been trained in another activity (Nishio, et al., 2018). For a new assignment, an already-trained model is used as the foundation (Al-Huseiny & Sajit, 2021). Machine Learning Applications from 2009. When data resources are restricted, this is a frequent technique in computer vision issues employing deep neural networks. As a consequence, I generate a starting point for new work by employing pre-trained models that have dealt with comparable problems in the past. Due to a limitation of sample volume, this technique is critical in medical image processing.

Pre-trained model's approach

A "Reuse Model" is one that uses a previously trained model as a starting point for a new model. This necessitates the incorporation of the complete model or its components. A widely used model may or may not need to be improved in the second procedure, which uses the new task's input-output data (Tymoshenko, & Moschitti, 2018). The third option is to choose one of the available models. Research institutes often publish algorithms that have been trained on difficult datasets, and they may completely or partially meet the challenge presented by a latest project.

VGG16 Architecture

Using fixed-size images, the 16-layer VGG convolutional network was created. A series of convolution layers with a 3x3 receptive field and small size pieces are used to process the data. This is the smallest scale on which up, down, right, left, and focus might be portrayed. There are extra 1x1 parts in the plan that can be named straight information change (trailed by nonlinearity) (Tejesh, Bhavana, V., & Krishnappa, 2022). The step of convolutions is fixed and set to 1 pixel (Number of pixels moved by each convolution divided by step size); as a result, in the wake of handling an info through a layer, the spatial goal remains something very similar, e.g., For 3x3 parts, the cushioning is fixed at 1. Five progressive pooling (max-pooling) layers, followed by a few convolution layers, are used to produce spatial shrinkage. Max-pooling, then again, doesn't have any significant bearing to every one of them. In a 2x2 pixel window with a 2-pixel step, the maximum pooling process happens (Papandreou, Kokkinos, & Savalle, 2015). Since it influences softmax to perform 1000-way characterization, Three Fully-Connected (FC) layers, the first two of which each have 4096 channels and the third of which has 1000 channels, are produced from this collection of convolutional layers (Shruthi, et al., 2023).

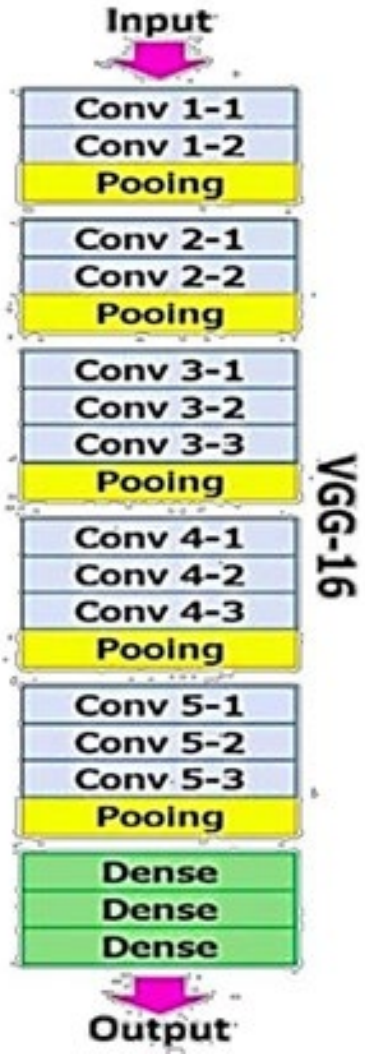

Figure 7. Image 3-1 VGG Network with 16 Layer

Residual Block

The mistake, for the most part, occurs as the number of layers in a convolutional neural network increases. Unfortunately, the opposite happens, with accuracy saturating and eventually decreasing. This is not due to over fitting but rather to a diminishing gradient. Due to the vanishing gradient problem, researchers were unable to develop deeper networks that performed better than their shallower counterparts. The fundamental idea underlying the ResNet model is to establish a "shortcut connection" (also known as a residual block or a skip connection) that bypasses one or more layers.

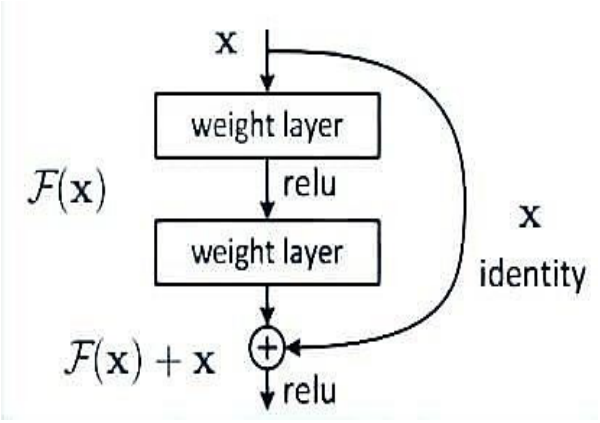

Figure 8. Residual Bloc

ResNet50 Architecture

Each phase of the ResNet-50 convolutional brain network consists of convolutions and personality blocks (Sahaai, et al., 2022). There are three convolutional layers in each convolution block. Figure 3.4 depicts an organization's architecture that is somewhat different (ResNet-34) (Deshpande, Estrela, & Patavardhan, 2021). The concept behind it is similar to its sibling model. Unlike ResNet-34, ResNet-50 replaces every two layers in a residual block with a three-layer bottleneck block and 1x1 convolutions, which reduces and then restores channel depth.

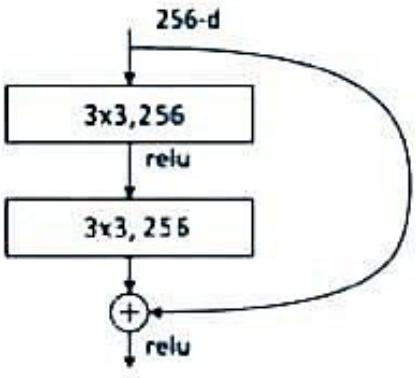

Figure 10. Channel Profundity

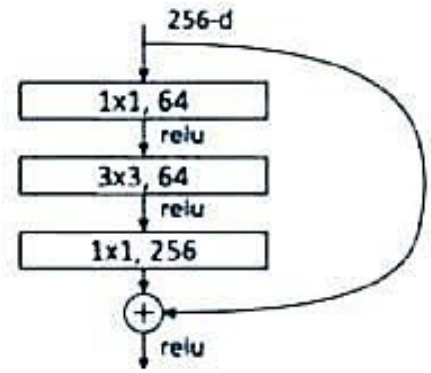

Figure 9. Convolutional of a 3x3 3-3.

Inception

Google specialists delivered the principal Inception (InceptionV1) brain network during the ImageNet contest in 2014 (Sadeghnezhad, & Salem, 2024). (See area 3.1.2). The model involved "beginning cell" obstructs that could direct convolutions utilizing a few scale channels prior to coordinating the outcomes into one. On account of 1x1 convolution, which diminishes the profundity of the information channel, the model recoveries estimations (Qian, 2018). Utilizing a progression of 1x1, 3x3, and in the end 5x5 size channels, a beginning unit cell figures out how to separate elements of different scales from the info picture. Despite the way that origin cells utilize the maximum pooling administrator, the component of handled information is protected due to the "same" course ding, which guarantees that the result is accurately linked (Uyulan, et al., 2021).

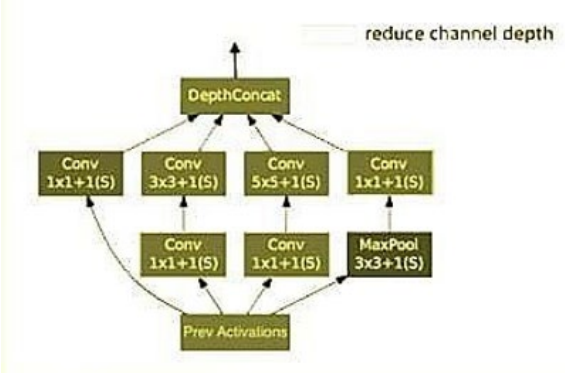

Figure 10. The First Model of Inception of Cell Introduced

Summary

This section provides a brief description of extreme learning machines, semi-supervised learning models, and an automated CXR screening system. Past profound learning approaches for Chest X-Ray investigation, aspiratory infection datasets, picture information expansion methods, and other arrangement result measurements are additionally talked about. The elements of profound convolutional brain networks in picture information examination are talked about.

Conclusion

Rather than relying on a small dataset, I used deep neural networks and segmentation to classify lung illnesses in my thesis work. When it came to understanding how our models worked, I looked at class activation maps. This research describes a number of deep learning architectures that competed in the ImageNet competition. Afterwards, these networks are used to train feature extractors for our low-level algorithms. The results are presented; I solely consider accuracy when assessing performance because the test set's distribution is uniform. A disease classification pipeline and the U-Net deep neural network. Segmentation of the X-ray images of the chest, prior to processing using the models outlined and then I compared the results obtained by training the same algorithms on a preprocessed dataset to those obtained by learning features from non-segmented photos. Additionally, I demonstrated how our solutions beat more complex models developed using the same data. As demonstrated in the thesis, segmentation enhances both the categorization logic and accuracy score. Because the highlighted parts may attract attention in the case of sick patients, networks are encouraged to only look into those areas of preprocessed Chest X-Ray images with remaining lungs, enhancing the interpretability of our models.

Acknowledgement

I would like to thank my Professor Hongwei Xie for her exceptional support during my studies after I must admire Jawad Ali for his efforts which he has put in my research.

Conflict of Interests

No conflict of interest.

References

Aherne, F. J., Thacker, N. A., & Rockett, P. I. (1998). The Bhattacharyya metric as an absolute similarity measure for frequency coded data. *Kybernetika*, *34*(4), 363-368.

Al-Huseiny, M. S., & Sajit, A. S. (2021). Transfer learning with GoogLeNet for detection of lung cancer. *Indonesian Journal of Electrical Engineering and computer science*, *22*(2), 1078-1086. https://doi.org/10.11591/IJEECS.V22.I2.PP1078-1086

Arbib, M. A. (Ed.). (2003). *The handbook of brain theory and neural networks*. MIT press.

Beylkin, G. (1987). Discrete radon transform. *IEEE transactions on acoustics, speech, and signal processing*, *35*(2), 162-172. https://doi.org/10.1109/TASSP.1987.1165108

Del Piccolo, N., Shirure, V. S., Bi, Y., Goedegebuure, S. P., Gholami, S., Hughes, C. C., ... & George, S. C. (2021). Tumor-on-chip modeling of organ-specific cancer and metastasis. *Advanced drug delivery reviews*, *175*, 113798. https://doi.org/10.1016/j.addr.2021.05.008

Deshpande, A., Estrela, V. V., & Patavardhan, P. (2021). The DCT-CNN-ResNet50 architecture to classify brain tumors with super-resolution, convolutional neural network, and the ResNet50. *Neuroscience Informatics*, *1*(4), 100013. https://doi.org/10.1016/j.neuri.2021.100013

Dhama, K., Chauhan, R. S., & Singhal, L. (2005). Anti-cancer activity of cow urine: current status and future directions. *International Journal of Cow Science*, *1*(2), 1-25.

Faguet, G. (2016). *Conquest of Cancer*. Springer.

He, K., Zhang, X., Ren, S., & Sun, J. (2016). Deep residual learning for image recognition. In *Proceedings of the IEEE conference on computer vision and pattern recognition* (pp. 770-778). https://doi.org/10.1109/cvpr.2016.90

Jaeger, S., Karargyris, A., Candemir, S., Folio, L., Siegelman, J., Callaghan, F., ... & McDonald, C. J. (2013). Automatic tuberculosis screening using chest radiographs. *IEEEtransactions on medical imaging*, *33*(2), 233-245. https://doi.org/10.1109/TMI.2013.2284099

Kostopoulos, G., Livieris, I. E., Kotsiantis, S., & Tampakas, V. (2018). CST-Voting: A semi-supervised ensemble method for classification problems. *Journal of Intelligent & Fuzzy Systems*, *35*(1), 99-109. http://dx.doi.org/10.3233/JIFS-169571

Krizhevsky, A., Sutskever, I., & Hinton, G. E. (2012). Imagenet classification with deep convolutional neural networks. *Advances in neural information processing systems*, *25*. https://doi.org/10.1145/3065386

Li, F., Arimura, H., Suzuki, K., Shiraishi, J., Li, Q., Abe, H., ... & Doi, K. (2005). Computer-aided detection of peripheral lung cancers missed at CT: ROC analyses without and with localization. *Radiology*, *237*(2), 684-690. https://doi.org/10.1148/radiol.2372041555

Liu, C., Yuen, J., & Torralba, A. (2010). Sift flow: Dense correspondence across scenes and its applications. *IEEE transactions on pattern analysis and machine intelligence*, *33*(5), 978-994. https://doi.org/10.1109/TPAMI.2010.147

Liu, Z., Zhong, J., Lyu, Y., Liu, K., Han, Y., Wang, L., & Liu, W. (2018, May). Location and fault detection of catenary support components based on deep learning. In *2018 IEEE International instrumentation and measurement technology conference (I2MTC)* (pp. 1-6). IEEE. https://doi.org/10.1109/I2MTC.2018.8409637

Lo, S. C. B., Chan, H. P., Lin, J. S., Li, H., Freedman, M. T., & Mun, S. K. (1995a). Artificial convolution neural network for medical image pattern recognition. *Neural networks*, *8*(7-8), 1201-1214.

https://doi.org/10.1016/0893-6080(95)00061-5

Lo, S. C., Lou, S. L., Lin, J. S., Freedman, M. T., Chien, M. V., & Mun, S. K. (1995b). Artificial convolution neural network techniques and applications for lung nodule detection. *IEEE transactions on medical imaging*, *14*(4), 711-718. https://doi.org/10.1109/42.476112

Loog, M., van Ginneken, B., & Schilham, A. M. (2006). Filter learning: application to suppression of bony structures from chest radiographs. *Medical image analysis*, *10*(6), 826-840. https://doi.org/10.1016/j.media.2006.06.002

Nebauer, C. (1998). Evaluation of convolutional neural networks for visual recognition. *IEEE transactions on neural networks*, *9*(4), 685-696. https://doi.org/10.1109/72.701181

Nery, R. (2012). *Cancer: An enigma in biology and society*. Springer Science & Business Media.

Nishio, M., Sugiyama, O., Yakami, M., Ueno, S., Kubo, T., Kuroda, T., & Togashi, K. (2018). Computer-aided diagnosis of lung nodule classification between benign nodule, primary lung cancer, and metastatic lung cancer at different image size using deep convolutional neural network with transfer learning. *PloS one*, *13*(7), e0200721. https://doi.org/10.1371/journal.pone.0200721

Oda, S., Awai, K., Suzuki, K., Yanaga, Y., Funama, Y., MacMahon, H., & Yamashita, Y. (2009). Performance of radiologists in detection of small pulmonary nodules on chest radiographs: effect of rib suppression with a massive-training artificial neural network. *American Journal of Roentgenology*, *193*(5), W397-W402. https://doi.org/10.2214/AJR.09.2431

Papandreou, G., Kokkinos, I., & Savalle, P. A. (2015). Modeling local and global deformations in deep learning: Epitomic convolution, multiple instance learning, and sliding window detection. In *Proceedings of the IEEE conference on computer vision and pattern recognition* (pp. 390-399). https://doi.org/10.1109/CVPR.2015.7298636

Pierce, G. B., & Damjanov, I. (1998). The pathology of cancer. *The biological basis of cancer*. Cambridge university press, Cambridge, UK, 14-49.

Qian, S. (2018). *Using convolutional neural network to generate neuro image template* (Master's thesis, The Ohio State University).

Ramalho, G. L. B., Rebouças Filho, P. P., Medeiros, F. N. S. D., & Cortez, P. C. (2014). Lung disease detection using feature extraction and extreme learning machine. *Revista Brasileira de Engenharia Biomédica*, *30*, 207-214. http://dx.doi.org/10.1590/rbeb.2014.019

Raza, A. (2019). *The First Cell: And the Human Costs of Pursuing Cancer to the Last*. Basic Books.

Sadeghnezhad, E., & Salem, S. (2024). InceptionCapsule: Inception-Resnet and CapsuleNet with self-attention for medical image Classification. *arXiv preprint arXiv:2402.02274*. https://doi.org/10.48550/arXiv.2402.02274

Sahaai, M. B., Jothilakshmi, G. R., Ravikumar, D., Prasath, R., & Singh, S. (2022, May). ResNet-50 based deep neural network using transfer learning for brain tumor classification. In *AIP Conference Proceedings* (Vol. 2463, No. 1). AIP Publishing. https://doi.org/10.1063/5.0082328

Shruthi, G., PM, K. R., Naidu, A. S., Kumari, A., Sravanti, C. H., & Gayathri, P. (2023, September). Detection of Lung Disease using Deep Learning Approaches. In *2023 International Conference on Network, Multimedia and Information Technology (NMITCON)* (pp. 1-8). IEEE. https://doi.org/10.1016/j.heliyon.2024.e26218

Suzuki, K. (2012). Pixel-based machine learning in medical imaging. *Journal of Biomedical Imaging*, *2012*, 1-5. https://doi.org/10.1155/2012/792079

Tejesh, S. S., Bhavana, V., & Krishnappa, H. K. (2022, December). Prediction of Mental Health of Aged Persons based on their Nervous System using Deep Learning Algorithms. In *2022 International Conference on Smart Generation Computing, Communication and Networking (SMART GENCON)* (pp. 1-5). IEEE.

https://doi.org/10.1109/SMARTGENCON56628.2022.10083869

Tymoshenko, K., & Moschitti, A. (2018). Shallow and deep syntactic/semantic structures for passage reranking in question-answering systems. *ACM Transactions on Information Systems (TOIS)*, *37*(1), 1-38. https://doi.org/10.1145/3233772

Uyulan, C., Ergüzel, T. T., Unubol, H., Cebi, M., Sayar, G. H., Nezhad Asad, M., & Tarhan, N. (2021). Major depressive disorder classification based on different convolutional neural network models: Deep learning approach. *Clinical EEG and neuroscience*, *52*(1), 38-51. https://doi.org/10.1177/1550059420916634

Warburg, O., & Nguyen, T. (2015). *The Prime Cause of Cancer* (Vol. 2). EnCognitive. com.